Journal of Alloys and Compounds 281 (1998) 264–267

Preparation and superconductivity of the quaternary alloy Mo–Ru–Rh–Pd

Jong-Gyu Lee*, Yong Joon Park, Jong Goo Kim, Kwang Yong Jee, Won Ho Kim

Korea Atomic Energy Research Institute, Nuclear Chemistry Laboratory, Yusong P.O. Box 105, Taejon 305-600, South Korea

Received 28 January 1998; received in revised form 14 March 1998

Abstract

Quaternary alloys with the nominal compositions of $Mo_{25}Ru_{50}Rh_{12.5}Pd_{12.5}$, $Mo_{30}Ru_{45}Rh_{12.5}Pd_{12.5}$, $Mo_{40}Ru_{40}Rh_{10}Pd_{10}$, and $Mo_{50}Ru_{20}Rh_{15}Pd_{15}$ were prepared using an Ar arc furnace. The structure of the alloys is isostructural to that of the ε-phase with a hexagonal close-packed structure. The secondary electron microscopic observation on the surface of alloys showed the formation of single crystalline microspheres with metallic luster. The measurements of magnetic susceptibility of the quaternary alloys, $Mo_{40}Ru_{40}Rh_{10}Pd_{10}$, and $Mo_{50}Ru_{20}Rh_{15}Pd_{15}$, showed the evidence of the superconducting transition at 3 and 5 K, respectively. The densities of the quaternary alloys are between 11.84–11.24 g cm^{-3}.

Keywords: Superconductivity; Alloy; insoluble residue; X-ray diffraction; Density

1. Introduction

The insoluble residue, an alloy consisting of Mo, Ru, Rh, Pd, Tc in spent nuclear fuel, has been considered important due to its insolubility in UO_2 [1,2]. The insoluble residue is formed as the fission products in a nuclear reactor and becomes the major natural resource of the Pt group metals, Pd, Rh and Ru, as the number of nuclear power plants increases [3]. It has often been observed in the form of spherical white inclusions in nuclear fuel rods through a microscope. The crystal size of the white inclusions is typically in the order of 5–10 μm and sometimes reaches ~30 μm when burn-up increases up to 11% [4]. The composition and structure of the white inclusions was identified by an electron probe microanalyzer (EPMA) and single crystal diffraction measurements in the 1960's [5]. One of the compositions determined by Bramman et al. was Mo–Tc–Ru–Pd (36:20:34:10) and has the structure of hexagonal close-packing (hcp) which has been well known as an ε-phase. It has the unit cell parameters, $a=2.73\pm0.02$ and $c=4.44\pm0.04$ Å. However, no spectroscopic and electromagnetic properties on the quaternary or quinary alloys Mo–(Tc)–Ru–Rh–Pd have been reported in detail since the first discovery in 1960's.

In this report, the preparation of the quaternary alloys, $Mo_{25}Ru_{50}Rh_{12.5}Pd_{12.5}$, $Mo_{30}Ru_{45}Rh_{12.5}Pd_{12.5}$, $Mo_{40}Ru_{40}Rh_{10}Pd_{10}$, and $Mo_{50}Ru_{20}Rh_{15}Pd_{15}$, are presented. The results of the powder X-ray diffraction (XRD), magnetic susceptibility and density measurements are also reported.

2. Experimental

The quaternary alloys, Mo–Ru–Rh–Pd (25:50:12.5:12.5, 30:45:12.5:12.5, 40:40:10:10, 50:20:15:15) were prepared using an Ar arc melting furnace (Ace Vacuum, Korea). The stoichiometric powdered mixture of Mo (Aldrich, 99.95%), Ru (Aldrich, 99.9%), Rh (Aldrich, 99.99%) and Pd (Aldrich, 99.9+%) was pelletized and completely melted three times by turning it upside down in the arc furnace.

An electron probe microanalyzer (EPMA, JEOL JXA-8600) was used to study the microstructure of the alloy. The wavelength dispersive X-ray (WDX) spectra were analyzed to determine the composition of the alloy.

The powder X-ray diffraction (Siemens D5000) patterns were recorded in the 2θ range of 30–90° with an internal standard Pt. The platinum wire on the alloy was pressed flat together in a hydraulic press.

The magnetic susceptibility of the alloys were measured with an applied magnetic field of 1000 G in the temperature range of 2–300 K using a SQUID magnetometer (Quantum Design). A pellet of the alloy with 70–150 mg was used for the measurements.

*Corresponding author.

0925-8388/98/$ – see front matter
PII: S0925-8388(98)00516-7

The densities of the alloys were measured in the distilled water using a pycnometer at room temperature (20.0°C). The volume (25 ml) of the pycnometer was calibrated at 20.0°C prior to the density measurements.

3. Results and discussion

The quaternary alloys, Mo–Ru–Rh–Pd (25:50:12.5:12.5, 30:45:12.5:12.5, 40:40:10:10, 50:20:15:15) were prepared successfully using an Ar arc furnace. The wavelength dispersive X-ray (WDX) analyses on several spots of the quaternary alloys resulted in the similar composition of Mo–Ru–Rh–Pd to the charged values (Table 1). Most of the elemental content of Mo, Ru, Rh and Pd in the quaternary alloys well matched the charged values within the experimental error ±10%. The relatively large deviation of mole% in $Mo_{40}Ru_{40}Rh_{10}Pd_{10}$ from the charged values might be due to the evaporation loss during arc melting as well as instrumental error. However, it showed a relatively good uniformity through the sample.

The powder XRD studies of the quaternary alloys resulted in the same hexagonal symmetry as the ε-phase reported previously in the literature (Fig. 1) [4,6]. In Fig. 1(d), the asterisk marks denote the impurity peaks of Mo, which are rarely observed. The unit cell parameters, *a* and *c* of the quaternary alloys Mo–Ru–Rh–Pd were obtained by least squares refinements based on the space group $P6_3/mmc$, which were 2.735–2.765 and 4.363–4.431 Å, respectively. As the Mo content in Mo–Ru–Rh–Pd increased, the unit cell parameters, *a* and *c*, almost linearly increased from 2.735 and 4.364 Å to 2.765 and 4.431 Å (Table 2). The powder XRD data of the quaternary alloys Mo–Ru–Rh–Pd are listed in Table 3.

We have also found that the structure of the quaternary alloys is similar to that of the binary alloys, $MoRh_3$ with 5.4538 and 4.3489 Å (S.G.$=P6_3/mmc$) and $MoRu_3$ with 5.4654(10) and 4.3423(9) Å [7], where two binary alloys were prepared in the same synthetic conditions. The a cell parameter of $MoRh_3$, known to have a Ni_3Sn-type structure [8], is almost double that of the ε-phase. The unit cell parameter *c* of the quaternary alloys Mo–Ru–Rh–Pd was greater than that of $MoRh_3$, 4.3489 Å. The increase of the c cell parameter seems to be due to the size effect upon the substitution of Rh by Mo and Ru in $MoRh_3$.

Table 1
The composition of the quaternary alloys from the analysis of wavelength dispersive X-ray spectra

	Mo (%)	Ru (%)	Rh (%)	Pd (%)
$Mo_{25}Ru_{50}Rh_{12.5}Pd_{12.5}$	26.2	48.5	13.1	12.2
$Mo_{30}Ru_{45}Rh_{12.5}Pd_{12.5}$	30.0	44.8	12.6	12.6
$Mo_{40}Ru_{40}Rh_{10}Pd_{10}$	42.2	40.2	9.4	8.2
$Mo_{50}Ru_{20}Rh_{15}Pd_{15}$	50.2	21.6	13.6	14.6

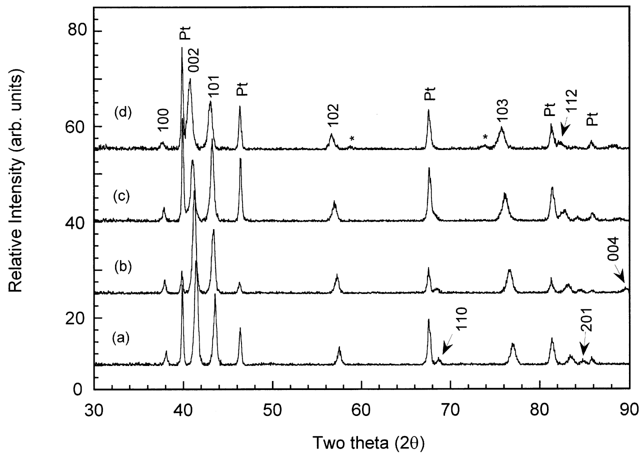

Fig. 1. Powder X-ray diffraction patterns of the quaternary alloys, (a) $Mo_{25}Ru_{50}Rh_{12.5}Pd_{12.5}$, (b) $Mo_{30}Ru_{45}Rh_{12.5}Pd_{12.5}$, (c) $Mo_{40}Ru_{40}Rh_{10}Pd_{10}$, and (d) $Mo_{50}Ru_{20}Rh_{15}Pd_{15}$. For $Mo_{50}Ru_{20}Rh_{15}Pd_{15}$, the asterisk mark denotes the Mo impurity.

Secondary electron microscopic (SEM) measurements on the surface of the alloys showed the existence of a spherical form of single crystals (Fig. 2). The spherical shape observed in the quaternary alloys were similar to the spherical white inclusions imbedded in the spent nuclear fuels of types such as Pressurized Water Reactor (PWR) and Fast Breeder Reactor (FBR).

The results of the magnetic susceptibility measurement of the quaternary alloys, $Mo_{40}Ru_{40}Rh_{10}Pd_{10}$ and $Mo_{50}Ru_{20}Rh_{15}Pd_{15}$ showed evidence of a superconducting transition at 3 and 5 K, respectively (Fig. 3a and b). In the χ (emu g^{-1}) vs. T plots of $Mo_{40}Ru_{40}Rh_{10}Pd_{10}$ and $Mo_{50}Ru_{20}Rh_{15}Pd_{15}$, the strong diamagnetic signals were shown to be below 3 and 5 K, respectively, suggesting the sharp superconducting transition. On the other hand, $Mo_{25}Ru_{50}Rh_{12.5}Pd_{12.5}$ and $Mo_{30}Ru_{45}Rh_{12.5}Pd_{12.5}$ do not show the diamagnetic signal. The observation of the superconducting transition in the quaternary alloys, $Mo_{40}Ru_{40}Rh_{10}Pd_{10}$ and $Mo_{50}Ru_{20}Rh_{15}Pd_{15}$, is not surprising, since several binary alloys with the same hcp structure such as MoRu, $Mo_{0.22}Ru_{0.8}$, MoRh and $Mo_{0.5}Pd_{0.5}$ showed a superconducting transition at 9.5–10.5, 1.66, 3.52 and 1.97 K, respectively [9]. In these quaternary alloys, the superconducting transition temperature also seems to be related to the relative Mo content in the alloy. From the above magnetic susceptibility data, the

Table 2
Variation of the unit cell parameters of quaternary alloys

	a (Å)	*b* (Å)	*V* ($Å^3$)
$Mo_{25}Ru_{50}Rh_{12.5}Pd_{12.5}$	2.735(1)	4.364(1)	28.25(1)
$Mo_{30}Ru_{45}Rh_{12.5}Pd_{12.5}$	2.742(1)	4.382(1)	28.54(2)
$Mo_{40}Ru_{40}Rh_{10}Pd_{10}$	2.753(1)	4.414(2)	28.98(2)
$Mo_{50}Ru_{20}Rh_{15}Pd_{15}$	2.765(3)	4.431(3)	29.33(4)

The space group(P63/mmc) of WRh_3 was used for the least squares refinements of the unit cell parameters.

Table 3
Powder x-ray diffraction data of quaternary alloys Mo-Ru-Rh-Pd

hkl	$Mo_{25}Ru_{50}Rh_{12.5}Pd_{12.5}$			$Mo_{30}Ru_{45}Rh_{12.5}Pd_{12.5}$			$Mo_{40}Ru_{40}Rh_{10}Pd_{10}$			$Mo_{50}Ru_{20}Rh_{15}Pd_{15}$		
	d_{calc} (Å)	d_{obs} (Å)	I/Io	d_{calc} (Å)	d_{obs} (Å)	I/Io	d_{calc} (Å)	d_{obs} (Å)	I/Io	d_{calc} (Å)	d_{obs} (Å)	I/Io
100	2.3678	2.3673	0.16	2.3748	2.3758	0.16	2.3844	2.3844	0.22	2.3943	2.4006	0.08
002	2.0822	2.0806	0.99	2.1911	2.1917	0.99	2.2070	2.2084	0.70	2.2155	2.2175	0.99
101	2.0812	1.6047	0.70	2.0879	2.0874	0.57	2.0979	2.0991	0.99	2.1064	2.1069	0.59
102	1.6046	1.6047	0.19	1.6104	1.6093	0.20	1.6197	1.6201	0.26	1.6261	1.6264	0.22
110	1.3670	1.3680	0.07	1.3711	1.3716	0.05	1.3766	1.3767	0.10	1.3823	1.3825	0.43
103	1.2395	1.2391	0.21	1.2442	1.2441	0.26	1.3521	1.2516	0.39	1.2570	1.2557	0.30
200	1.1839	*	<0.02	1.1874	-	<0.02	1.1922	–	<0.02	1.1971	–	<0.02
112	1.1585	1.1587	0.10	1.1623	1.1621	0.07	1.1680	1.1673	0.10	1.1728	1.1729	0.12
201	1.1426	1.1430	0.03	1.1461	1.1476	0.03	1.1509	1.1504	0.05	1.1557	1.1549	0.02

*The peak position of 200 was not determined due to weak intensity.

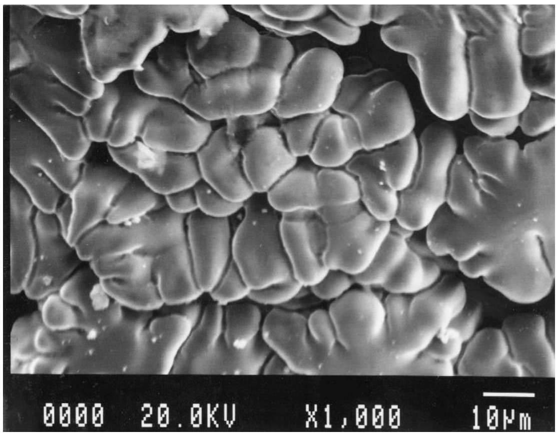

Fig. 2. SEM image of the quaternary alloy $Mo_{40}Ru_{40}Rh_{10}Pd_{10}$.

Mo content of 25–35% in the Mo–Ru–Rh–Pd system does not produce any superconducting phase showing a transition above 2 K. A further confirmation on the superconducting transition in these phases should be followed by measurements of the electrical resistivity at low temperatures.

The density measurements of the quaternary alloys resulted in values of 11.24–11.84 g cm^{-3} (Table 4). The density of the alloys decreased from 11.84 to 11.24 g cm^{-3} as the Mo content increased from 25 to 50 mol %. The measured densities of the quaternary alloys well-matched the calculated values based on the unit cell volumes from the XRD data within an error less than 2%.

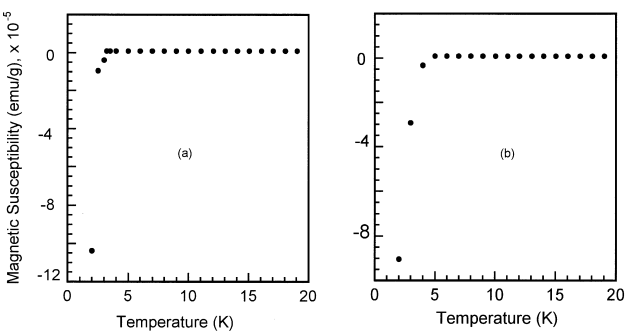

Fig. 3. Superconducting transition of the quaternary alloys, (a) $Mo_{40}Ru_{40}Rh_{10}Pd_{10}$ and (b) $Mo_{50}Ru_{20}Rh_{15}Pd_{15}$. The susceptibility was measured in the applied magnetic field of 1000 Gauss during warming after cooling in the zero magnetic field.

Table 4
The density of the quaternary alloys

	d_{obs} (g cm^{-3})	d_{calc} (g cm^{-3})[a]
$Mo_{25}Ru_{50}Rh_{12.5}Pd_{12.5}$	11.84(14)	11.82
$Mo_{30}Ru_{45}Rh_{12.5}Pd_{12.5}$	11.74(14)	11.68
$Mo_{40}Ru_{40}Rh_{10}Pd_{10}$	11.54(14)	11.40
$Mo_{50}Ru_{20}Rh_{15}Pd_{15}$	11.24(14)	11.27

The pycnometer was calibrated at 20.0°C.
[a] The calculated density values were obtained from the experimental composition by EPMA measurements.

4. Conclusion

The quaternary alloys, known as an ε-phase, were prepared using an Ar arc melting furnace. The unit cell parameters a and c were refined by a least squares method based on the space group $P6_3/mmc$. The a cell parameter of quaternary alloys is approximately half that of $MoRh_3$, a binary alloy with the same hcp structure. SEM image of the alloys revealed the existence of single crystalline microspheres with metallic luster. The magnetic susceptibility measurements of the quaternary alloys, $Mo_{40}Ru_{40}Rh_{10}Pd_{10}$, and $Mo_{50}Ru_{20}Rh_{15}Pd_{15}$ showed the evidence of the superconducting transition at 3 and 5 K, respectively. Above the transition temperature, it showed a typical Pauli-paramagnetic behavior. The density of the quaternary alloys falls in the range of 11.84–11.24 g cm^{-3}.

Acknowledgements

The authors greatly acknowledge the financial support (Nuclear Development Fund) from the Korea Ministry of

Science and Technology. We also thank Mr. Kyu Won Lee for the magnetic susceptibility measurements and Mr. Soon Dal Park for the electron probe microanalyses.

References

[1] T. Matsui, M. Ohkawa, R. Sasaki, K. Naito, J. Nucl. Mater. 200 (1993) 11.
[2] T. Adachi, M. Ohnuki, N. Yoshida, T. Sonobe, W. Kawamura, H. Takeishi, K. Gunji, T. Kimura, T. Suzuki, Y. Nakahara, T. Muromura, Y. Kobayashi, H. Okashita, T. Yamamoto, J. Nucl. Mater. 174 (1990) 60.
[3] K. Naito, T. Matsui, Y. Tanaka, J. Nucl. Sci. Technol. 23(6) (1986) 540.
[4] H. Kleykamp, Nucl. Technol. 80 (1988) 412.
[5] J.I. Bramman, R.M. Sharpe, D. Thom, G. Yates, J. Nucl. Mater. 25 (1968) 201.
[6] J. Octavio, A. Paschoal, J. Kleikamp, F. Thummler, Z. Metallkde 74 (1983) 652.
[7] Yong Joon Park, Jong-Gyu Lee, Jong Goo Kim, Jung Seok Kim and Kwang Yong Jee, Analytical Science and Technology 11(3) (1998).
[8] P. Villars, L.D. Calvert, (Eds.), Pearson's Handbook of Crystallographic Data for Intermetallic Phases, 2nd Ed., Vol. 4, 1991, p. 5092.
[9] R.C. Weast, (Ed.), CRC Handbok of Chemistry and Physics, 70th Ed., E-98 (1989–1990).